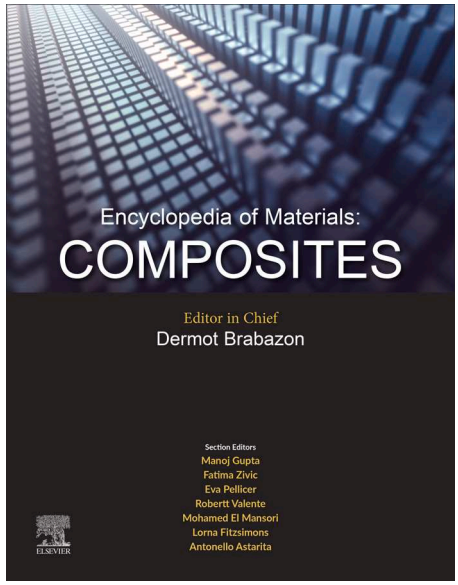

Nicolenco, Aliona, Navarro-Senent, Cristina and Sort, Jordi (2021) Nanoporous Composites With Converse Magnetoelectric Effects for Energy-Efficient Applications. In: Brabazon, Dermot (ed) Encyclopedia of Materials: Composites. vol. 2, pp. 450–460. Oxford: Elsevier.

http://dx.doi.org/10.1016/B978-0-12-803581-8.11870-3

Nanoporous Composites With Converse Magnetoelectric Effects for Energy-Efficient Applications

Aliona Nicolenco, Autonomous University of Barcelona, Barcelona, Spain and Institute of Applied Physics, Chisinau, Moldova
Cristina Navarro-Senent, Autonomous University of Barcelona, Barcelona, Spain
Jordi Sort, Autonomous University of Barcelona, Barcelona, Spain

Nomenclature

ALD Atomic layer deposition
BTO Barium titanate, $BaTiO_3$
CME Converse magnetoelectric effect
DME Direct magnetoelectric effect
EISA Evaporation induced self-assembly
FE Ferroelectric
FM Ferromagnetic
ME Magnetoelectric
MOKE Magneto-optic Kerr effect
PC Propylene carbonate
PMN-PT Lead magnesium niobate-lead titanate, $Pb(Mg_{1/3}Nb_{2/3})O_3$–$PbTiO_3$
PZT Lead zirconate titanate, $Pb[Zr_{(x)}Ti_{(1-x)}]O_3$
SQUID Superconducting quantum interference device
VSM Vibrating sample magnetometry

Glossary

Converse magnetoelectric effect Modulation of magnetic properties in magnetic materials by means of external electric field.
Direct magnetoelectric effect Modulation of electric polarization in dielectric materials by external magnetic fields.
Joule heating effect Energy dissipation induced by electrical currents flowing through a resistor.
Magnetoelectric composites Heterostructures which comprise magnetic and dielectric counterparts in which the properties of the magnetic material can be manipulated with voltage, either using solid or liquid electrolytes.
Magneto-ionics Magnetoelectric mechanism in which the oxidation state of the metal in the magnetic phase is influenced by the ions (e.g., O^{2-}) diffusion back and/or forth from the material of interest toward an ion source/sink (e.g., a high O^{2-} mobility thin film, deposited next to the magnetic layer), depending on the voltage polarity.
Magnetostriction Ability of most ferromagnetic materials to expand or contract in response to an external magnetic field.
Single-phase multiferroics Materials possessing an inherent coupling between magnetic and electric orders.
Spinels A class of material, which crystallizes in the cubic crystal system, with general formula AB_2X_4, where A and B are cations of (II) or (III) valent element (or the same element, as in Fe_3O_4) and X is an anion (typically oxygen or sulfur).

Introduction

Magnetism and electricity have always had an intimate link. Particularly interesting is the coexistence of magnetic and electric orders in magnetoelectric (ME) materials which makes them able to respond, simultaneously, to external magnetic and electric stimuli: (1) Electric polarization can be modulated by external magnetic fields (direct ME effect, DME) and (2) magnetic properties can be largely controlled with an electric field (converse ME effect, CME) (Wang *et al.*, 2010; Hu and Nan, 2019). In conventional ME composites, coupling between piezoelectric/ferroelectric (FE) and ferromagnetic (FM) constituents is mediated by strain and, in some cases, by electric charge effects (Wang *et al.*, 2010; Hu and Nan, 2019; Molinari *et al.*, 2019; Navarro-Senent *et al.*, 2019). In recent years, progress has been made in the so-called magneto-ionic heterostructures, where voltage-driven magnetic changes are mediated by ion migration/intercalation (typically O^{2-}, Li^+ (Dasgupta *et al.*, 2014; Zhang *et al.*, 2016) or H^+ species (Tan *et al.*, 2019)) (Bauer *et al.*, 2015; Duschek *et al.*, 2016; Gilbert *et al.*, 2016). DME effects are appealing for healthcare technologies (Chen *et al.*, 2017), water remediation systems (Mushtaq *et al.*, 2019a,b) and sensors/actuators (Wang *et al.*, 2010), whereas CME effects can be exploited in microelectromechanical systems and energy-efficient magnetic memories (Peng *et al.*, 2016).

Unfortunately, in FM films directly grown onto FE substrates, the voltage required to generate ME effects is extremely high (e.g., 4 kV) (Ahmad *et al.*, 2015) due to the large thickness of the substrate (i.e., in capacitors, electric field is inversely proportional to the dielectric thickness). This is not suitable for microelectronics, where much lower voltages (<10 V) are desirable to enhance energy efficiency and not to burn the electronic components. If thin FE/FM bilayers directly grown onto rigid (non-FE) substrates, then the required voltages are lower, but the attainable strain is small due to the clamping with the substrate, thus also limiting the extent of ME effects (Torah *et al.*, 2004; Schmitz-Antoniak *et al.*, 2013; Chien *et al.*, 2016). To overcome these drawbacks, new ME composites based on nanoporous materials filled with either liquid or solid dielectric materials (eventually FE polymers) have been recently developed. These types of materials are overviewed in this article.

During the last two decades, much progress has been made in the synthetic procedures to prepare nanoporous systems with precise control of the porosity degree, pore/ligament sizes and crystallinity of the pore walls. This development has been triggered by the widespread use of these materials in chemistry areas such as catalysis, gas sensors, or supercapacitors, where a high surface-to-volume ratio (S/V) favors an enhanced performance. Also remarkable is the literature dealing with the growth and characterization of mesoporous composites containing embedded ferromagnetic particles, to be used in drug delivery applications (Trewyn *et al.*, 2007), ultra-light magnets (Heiligtag *et al.*, 2014) or water remediation (Kharissova *et al.*, 2015). Interestingly, although many of the cutting-edge technological applications in nanomagnetism/spintronics also rely on surface or interface magnetic phenomena (e.g., spring-magnets, exchange bias, skyrmions, etc.) (Bibes *et al.*, 2011), the use of nanoporous materials in this field has been mainly overlooked.

In the particular subject of voltage-driven magnetic actuation, the study of nanoporous materials (i.e., mesoporous metals or oxides filled with a liquid high dielectric constant, or metal/metal oxide porous nanocomposites), all with high S/V ratio, is relatively new. In such materials, the relatively small effects from seminal works on magnetoelectric phenomena, initially observed in ultra-thin metallic films (Weisheit *et al.*, 2007), are drastically enhanced (Molinari *et al.*, 2018; Navarro-Senent *et al.*, 2019). In fact, it is easy to calculate that the S/V ratio of a 50-nm-thick porous film covering an area of $1 \times 1\ \mu m^2$ and being made of a square array of vertically oriented cylindrical pores, with 5 nm pore diameter and 2.5 nm average pore wall (i.e., $\sim$50% total porosity) is about 40 times larger than the S/V ratio of a fully dense layer of 50 nm thickness. Hence, the voltage-driven magnetic interfacial effects that depend on the S/V ratio (i.e., magnetic anisotropy, coercivity, direction of the magnetization, exchange bias), as well as those proportional to the total volume of affected material (e.g., the net magnetic moment) can be significantly enhanced in the porous architecture, by several orders of magnitude, with respect to non-porous magnetic thin films.

To measure the CME in nanoporous materials, either conventional magnetometry (vibrating sample or SQUID magnetometers) or magneto-optic Kerr effect techniques, in conjunction with custom-made setups to apply voltage, can be utilized (see **Fig. 1**). Either solid dielectrics (prepared by, e.g., atomic layer deposition) or liquid electrolytes, which form the so-called electric double layer upon voltage application, can be used.

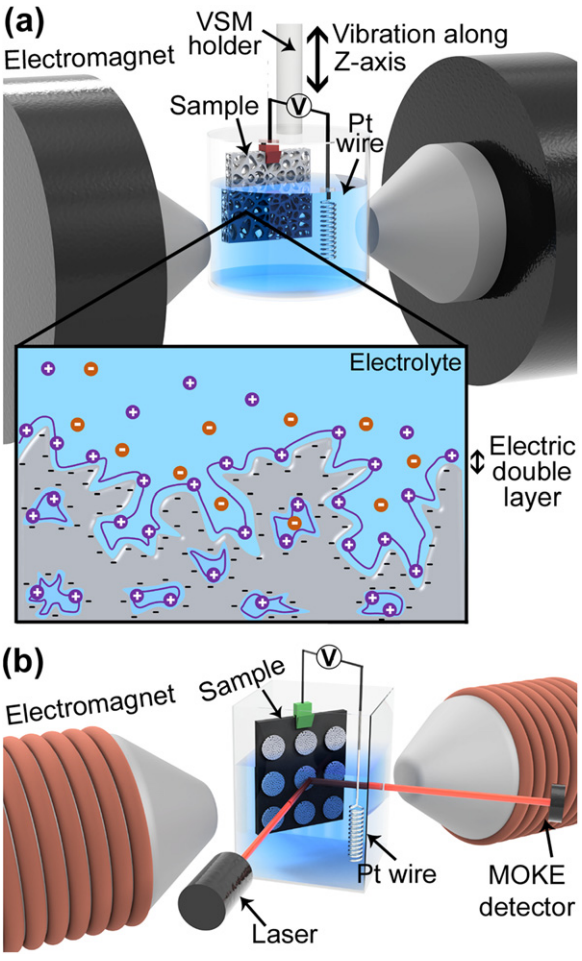

Fig. 1 Schematic illustration of the experimental setups typically used for magnetoelectric measurements in liquid configuration using (a) a vibrating sample magnetometer (VSM) and (b) a magneto-optic Kerr effect setup (MOKE).

The main body of this article is divided into three sections, covering CME in (1) metal-based composites, (2) metal/metal oxide systems and (3) all-oxide heterostructures, all based on nanoporous architectures. Here the use of the "composite" term is extended (as in the review paper by Molinari *et al.*, 2019) to include those materials comprising a nanoporous framework filled with either a solid or a liquid second phase (often needed to generate the electric field or as buffer materials for magneto-ionics). We begin each section with a short introduction on the growth methods and experimental procedures used to induce and control the nanoporosity. We then focus on the most recent progress on the nanoporous ME composites belonging to each of the three categories, with emphasis on the systems where the ME effects are exacerbated due to the presence of nanoporosity. The article is followed by brief concluding remarks and perspectives.

Magnetoelectric Composites Based on Nanoporous Metals or Metal Alloys

Based on previous works on magnetism tuned by carrier density modulation in thin film magnetic semiconductors (Ohno *et al.*, 2000; Chiba *et al.*, 2003), as well as preliminary theoretical works that predicted a strong dependence of the magnetic anisotropy energy on the number of valence band electrons in alloys such as Fe–Pt or Co–Pt (Daalderop *et al.*, 1991), Weisheit *et al.* demonstrated in 2007 that the coercivity of ultra-thin Fe–Pt and Fe–Pd films could be modified by up to 4.5% under the action of external voltage during electrolyte gating (Weisheit *et al.*, 2007). Since electric field in metals is confined within the Thomas–Fermi screening length (which is of the order of 0.5 nm), the changes in coercivity driven by voltage in metallic alloys were initially only observed in films of $2-3$ nm in thickness.

In parallel to these works on ultra-thin metallic films, Weïssmuller *et al.* showed that reversible changes in strain could be induced in nanoporous Pt due to electric surface charge accumulation (Weissmüller *et al.*, 2003). Further investigations in that direction revealed that the magnetic susceptibility of nanoporous Pd (Drings *et al.*, 2006) and the ferromagnetic properties of Pd–Co (Ghosh *et al.*, 2006), Pd–Ni (Ghosh, 2011, 2013) and Au–Fe (Mishra *et al.*, 2010) nanoporous alloys could be also manipulated with voltage due to these electrically induced variations of strain. In these works, the typical size of the crystallites comprised in the porous frameworks ranged between 8 and 20 nm. The charge-induced pressure on the nanocrystallites comprised in the nanoporous frameworks and the concomitant changes in sample dimensions during electrochemical charging and discharging processes were found to be responsible for these observations. In spite of their fundamental interest, the typical changes in magnetization due to strain effects are usually rather small (up to 0.5% at room temperature and 3% near the Curie temperature; Ghosh *et al.*, 2006). An interesting theoretical work by Subkow and Fähnle (2011) analyzed in detail the effects of (1) filling of the electronic *d* band upon electric charging and (2) the magnetoelastic response to charge-induced strain variations in the nanoparticles forming nanoporous systems, both of which play a role during magnetoelectric actuation of these metallic alloys using liquid electrolytes. The authors concluded that the magnetic anisotropy energy of this type of systems can be modified with voltage only at the surface of nanoparticles (constituting the nanoporous framework) that are not in grain–boundary contact, which are the ones that can be effectively charged in the electrolyte due to the formation of the electric double layer when voltage is applied.

Subsequent works have been carried out to try to enhance the effects of voltage in the magnetic properties of nanoporous metallic alloys. Different experimental techniques have been used to improve the quality of the synthesized materials (i.e., to reduce the pore wall width or ligament size, or to make the porosity pseudo-ordered). Some of the most standard methods include micelle-assisted electrodeposition, electrochemical dealloying, or electrodeposition combined with colloidal templating (see **Fig. 2**).

Electrochemical dealloying is a method that allows fabricating porous films from previously deposited fully dense counterparts. In this case, the porous metal or metal alloy is obtained by selectively dissolving the most electrochemically active element comprised in an alloy. This technique has been shown successful to generate porosity in bulk metals, ribbons, as well as thin films (the latter grown by, e.g., electrodeposition or sputtering, as in the example shown in **Fig. 2(a)**) (Sun *et al.*, 2004; Robbennolt *et al.*, 2018). Colloidal templating is a facile and cost-effective method to create well-defined, pseudo-ordered 3D porous structures by using 3D assembled nanospheres as a soft mask (Dislaki *et al.*, 2018). Colloid size and self-assembly are factors that determine the nanopore dimensions, pore wall width and overall layer thickness (see **Fig. 2(b)**). Various methods to assemble monodisperse micro- and nanospheres have been put forward in the literature, such as dip coating, spin-coating, self-assembly, solvent evaporation, or electrophoresis. Among these methods, electrophoretic deposition is amongst the most attractive options for achieving homogeneous coverage of close-packed arrangements of spheres. Finally, micelle-assisted electrodeposition relies on the formation of micelles in the electrolytic bath which act as soft templates (structure-directing agents) during the growth of the metallic layers of interest. When a block co-polymer (e.g., P123) is added to the electrolyte at a concentration above "critical micelle concentration," micelles start to form spontaneously in the solution, getting progressively in contact and tending to self-assemble at the solid–liquid interface (Quintana *et al.*, 2017; Isarain-Chávez *et al.*, 2018; Li *et al.*, 2018). When voltage is applied to the cathode and reduction of the metal cations takes place, these micelles interfere and guide the electrodeposition process, leading to the growth of mesoporous metallic films (see **Fig. 2(c)**). The pore size (and pore wall size) is typically very small (even sub-5 nm). If the surfactant concentration is high enough to form a lyotropic liquid crystal, regular arrangements of pores can be obtained.

Remarkably, using this structure-optimized nanoporous alloys, changes up to 32% in coercivity (with virtually no significant variations in the saturation magnetization) have been reported in recent years in relatively thick films (0.5–1 μm) of various alloy compositions (nanoporous Cu–Ni, Co–Pt, Fe–Cu), mainly due to changes in the magnetic anisotropy energy stemming from electric surface charge accumulation, as evidenced by ab-initio calculations (Quintana *et al.*, 2017). Depending on the alloy system,

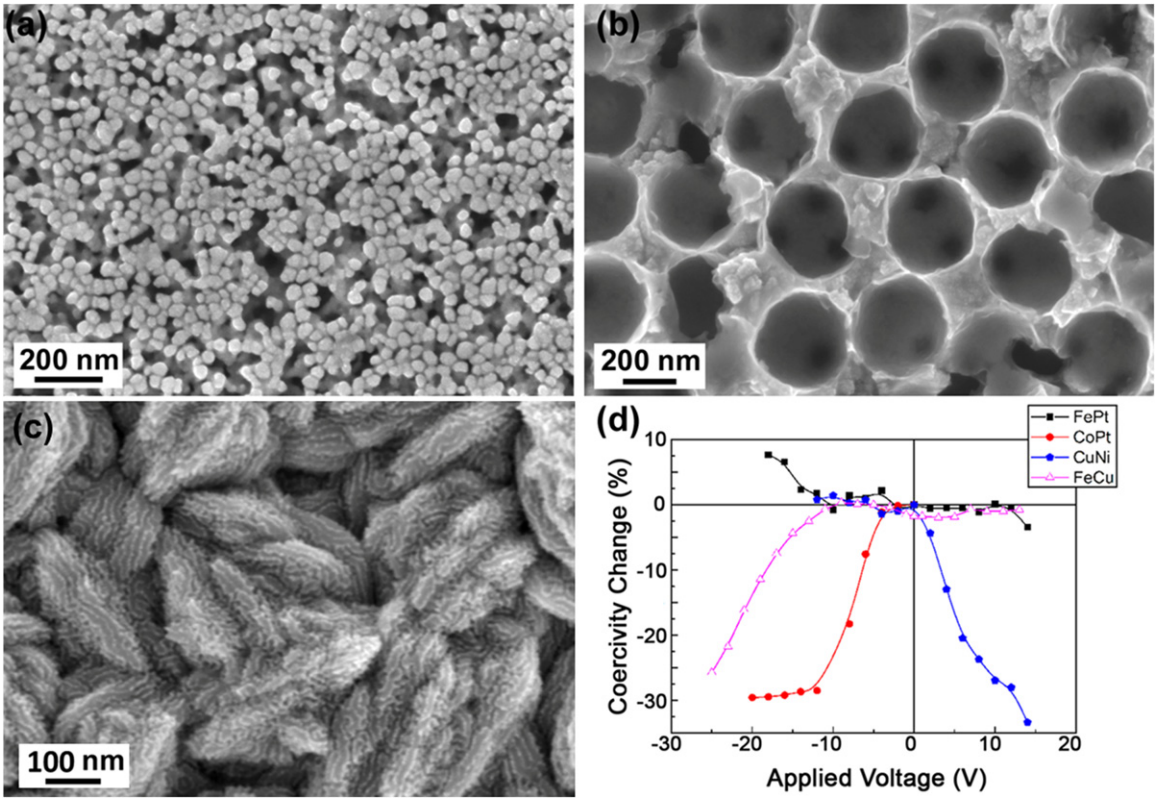

Fig. 2 Representative scanning electron microscopy (SEM) on-top images of (a) dealloyed Fe–Cu sputtered films, (b) electrodeposited Fe–Cu porous films grown onto colloidal templated substrates, (c) nanoporous Co–Pt films prepared by micelle-assisted electrodeposition. Panel (d) shows the relative variations of coercivity, as function of voltage, in various porous alloys electrolyte-gated using an anhydrous electrolyte (propylene carbonate). In all these cases, the voltage effects are mainly due to surface charge accumulation. Reprinted from (d) Navarro-Senent, C., Quintana, A., Menéndez, E., Pellicer, E., Sort, J., 2019. Electrolyte-gated magnetoelectric actuation: Phenomenology, materials, mechanisms, and prospective applications. APL Materials 7 (3), 030701. doi:10.1063/1.5080284.

the coercivity can either increase or decrease for either positive or negative applied voltages (**Fig. 2(d)**). Also, the changes in coercivity as a function of voltage polarity are often not symmetric. This can be due to the way the magnetic anisotropy energy varies with the electric field or because of the dissimilar thickness (and nature) of the electric double layer formed at the interfaces between the pore walls and the electrolyte during positive/negative voltage application. The experimental demonstration that the coercivity of thick nanoporous magnetic alloy films can be drastically reduced by simply subjecting this type of materials to the action of an electric field (i.e., applying a moderate DC voltage to them) is very appealing for energy-efficient magnetic actuation. If the coercivity is reduced, lower magnetic fields are needed to induce magnetization reversal (i.e., to write the magnetic bits of information in memory devices). As a consequence, less electric current is required, and this concurrently lowers undesirable Joule heating effects. The large S/V ratio and the ultra-narrow pore walls of these systems play a crucial role in the observed effects. Since electric field in metals is confined at their surface, the nanoporous morphology of the investigated materials allows for much larger accumulation of electrostatic charges compared to fully-dense films. That is, the whole nanoporous structure is affected by the electric field and not only the outer topmost surface, thus resulting in a very significant voltage-induced reduction of coercivity. This waives the stringent "ultrathin-film requirement" from previous studies, wherein smaller voltage-driven coercivity variations were reported (Weisheit *et al.*, 2007). Finally, besides coercivity, tuning of the superparamagnetic state has been achieved in nanoporous Co–Pd alloys electrically gated in a 1 M aqueous KOH electrolyte (Gößler *et al.*, 2019). The effect seems to be related to electrochemical hydrogen sorption. More specifically, a strong magneto-ionic (H^+) effect arises from coupling of the magnetic clusters via a Ruderman–Kittel–Kasuya–Yoshida-type interaction in the Pd matrix which is enhanced by the hydrogen sorption.

An overview of the different types of electrolytes, materials and main magnetoelectric effects observed in nanoporous metallic alloys, metal/metal oxide composites and pure oxide systems is given in **Table 1**.

Magnetoelectric Composites Based on Nanoporous Metal/Metal Oxide Heterostructures

In most of the examples discussed in the previous section, an anhydrous electrolyte (e.g., propylene carbonate) was utilized in order to induce electric charge accumulation at the surface of nanoporous metallic alloys (through the formation of the

Table 1 Representative materials, typical electrolytes and most prominent magnetoelectric effects induced in nanoporous materials with voltage (electrolyte-gating)

Electrolyte	*Material*	*Variation*	*Reversibility*	*References*
$LiClO_4$ in EC	Nanoporous Au–Fe alloy	M = 0.2%	Yes	Mishra *et al.* (2010)
$LiClO_4$ in EC	Nanoporous Pd–Ni alloy	M ≈ 0.5%	Partially (ΔV, ∼1 h) Yes (ΔV, ∼1 h)	Ghosh (2011)
PC	Nanoporous Cu–Ni film	H_C = −32%	–	Quintana *et al.* (2017)
PC	Pseudo-ordered porous Fe–Cu film	H_C = −25%	Partially (0 V, 5 min)	Dislaki *et al.* (2018)
$LiClO_4$ in EC	Nanoporous Pd–Co alloy	M = 3%	Partially (ΔV, ∼2 h)	Ghosh *et al.* (2006)
1 M KOH	Nanoporous Pd–Ni alloy	M = 24.6%	Yes (ΔV, ∼2 h)	Ghosh (2013)
1 M KOH	Nanoporous Co–Pd alloy	M = 100% (ON–OFF)	Yes (ΔV, ∼ h)	Gößler *et al.* (2019)
1 M NaOH	Nanoporous Cu–Ni	M_S = +33%	Yes (ΔV, 10 min)	Quintana *et al.* (2018a)
PC	Nanoporous Co–Pt lithographed disks	ΔM_S = 66% ΔH_C = −88%	Partially (DV, ∼ min)	Navarro-Senent *et al.* (2018)
PC	Nanoporous Co–Pt + HfO_2/Al_2O_3 films	Δm_S = 76% ΔH_C = −58%	Partially (ΔV, ∼2 h)	Navarro-Senent *et al.* (2020)
1 M KOH	Porous γ-Fe_2O_3/Pt-nanocomposite	Δm = 10.4%	Yes (ΔV, ∼5 min)	Topolovec *et al.* (2013)
LiTFSI in EMIM-TFSI	Nanoporous $Co_{0.5}Ni_{0.5}Fe_2O_4$ and $CoFe_2O_4$ films	ΔM ≈ 2–5%	Yes (ΔV, ∼ min)	Dubraja *et al.* (2018)
LiTFSI in EMIM-TFSI	Nanoporous $LiFe_5O_8$ films	ΔM ≈ 4%	Yes (ΔV, ∼ h)	Reitz *et al.* (2016)
PC	Nanoporous Fe–Cu films	ΔM_S = 20% ΔH_C = 100%	Partially (ΔV, 40 min)	Robbennolt *et al.* (2018)
PC	Nanoporous $CoFe_2O_4$ films	ΔM_S = 15% ΔH_C = +28%	Yes (ΔV, ∼2 h)	Robbennolt *et al.* (2019a)
PC	Nanoporous $CoFe_2O_4$ + HfO_2 films	ΔM_S = +56% ΔH_C = + 69%	Yes (ΔV, ∼1 h)	Robbennolt *et al.* (2020)
PC	Nanoporous FeO_x films	ΔM_S = 1310% ΔH_C = +100%	Partially (ΔV, ∼1 h)	Robbennolt *et al.* (2019b)

Abbreviation: EC, ethylene carbonate; EMIM-TFSI, 1-ethyl-3-methylimidazolium bis(trifluoromethylsulfonyl)imide; H_C, coercivity; LiTFSI, lithium bis(trifluoromethanesulfonyl)imid; m, magnetic moment; M, magnetization; M_S, saturation magnetization; PC, propylene carbonate.
Note: Table adapted from Navarro-Senent, C., Quintana, A., Menéndez, E., Pellicer, E., Sort, J., 2019. Electrolyte-gated magnetoelectric actuation: Phenomenology, materials, mechanisms, and prospective applications. APL Materials 7 (3), 030701. doi:10.1063/1.5080284.

electric double layer). As aforementioned, this causes electric field induced changes in the magnetic properties (converse magnetoelectric effect), which are often reversible. In some cases, though, an aqueous electrolyte (e.g., 1 M KOH or NaOH) has been purposely utilized in the literature to trigger reduction–oxidation electrochemical reactions at the surface of the metallic porous frameworks or in metal/metal oxide islands when voltage is applied (Duschek *et al.*, 2018; Quintana *et al.*, 2018a). Sometimes, unexpected results have been encountered. For example, when positive voltage is applied to electrodeposited nanoporous Cu-Ni alloys and the films get oxidized, an increase (rather than a decrease) of the saturation magnetization is observed (Quintana *et al.*, 2018a). This counter-intuitive result can be understood because of the preference for Cu (rather than Ni) to get selectively oxidized. As a consequence, upon application of a positive voltage, the Cu–Ni alloy gets progressively enriched in Ni (as Cu is oxidized) and the resulting magnetic moment increases. The process can be fully reversed by application of a negative voltage. Oxygen migration can also cause changes in the coercivity of the nanoporous alloy, as well as in the perpendicular magnetic anisotropy (Ibrahim *et al.*, 2018). However, in nanoporous systems, since shape anisotropy is not clearly defined (i.e., these materials are typically polycrystalline and the ligaments and pore walls are randomly oriented), no pronounced anisotropy effects are typically reported.

Some nanocomposite porous materials contain oxide phases in the as-prepared states (as depicted in **Fig. 3**) (Navarro-Senent *et al.*, 2018; Robbennolt *et al.*, 2018). Some examples are nanoporous Co–Pt + CoO_x lithographed disks prepared by electrodeposition or nanoporous Fe–Cu + FeO_x + CuO_y films prepared by electrochemical dealloying. In these cases, migration of the structural oxygen (i.e., oxygen present in the as-prepared material) can occur when voltage is applied, even when utilizing anhydrous electrolytes, thereby rendering truly magneto-ionic effects (Navarro-Senent *et al.*, 2018). When this occurs, drastic changes in the coercivity and the magnetic moment at saturation take place. In some cases (e.g., nanoporous Fe–Cu solid solutions), this oxygen migration causes structural transformations in the metallic counterpart (e.g., from Cu-rich face centered cubic to Fe-rich body centered cubic phases) (Robbennolt *et al.*, 2018). Eventually, ON-OFF transitions (reversible transformations from ferromagnetic to paramagnetic or antiferromagnetic states) might be induced in nanoporous metal + metal oxide thin films, similar to what has been observed in nanostructured oxide thin films (Duschek *et al.*, 2018; Quintana *et al.*, 2018b).

Another effect that could be of interest in this type of nanocomposites would be the study of the eventual exchange bias phenomenon (i.e., shift of the hysteresis loop, along the magnetic field axis, due to the coupling between ferromagnetic and the electrochemically generated antiferromagnetic or ferrimagnetic phases). While this has been studied in flat, non-porous, multilayered films (Gilbert *et al.*, 2016; Zhou *et al.*, 2016), comprehensive studies in nanoporous composites have not yet been reported.

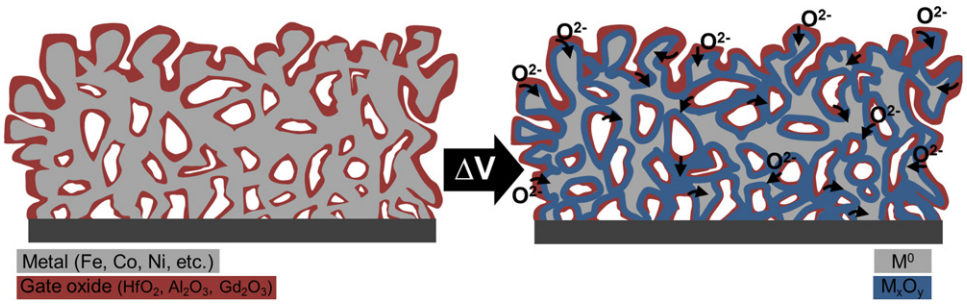

Fig. 3 Schematic drawing of voltage-induced oxygen migration in metal (M)/metal oxide (M_xO_y) magnetoelectric composite under the action of an applied voltage, ΔV.

All-Oxide Nanoporous Magnetoelectric Composites

Up to date, the vast majority of magnetoelectric studies (in liquid and solid state) have been performed in oxide systems. As a matter of fact, all intrinsic multiferroics are oxides, for example, spinels (Fe_3O_4, $CoFe_3O_4$), perovskites ($BiFeO_3$, $BaTiO_3$) (Liu and Yang, 2017) and hexagonal manganites ($RMnO_3$, where R is a rare-earth element) (Vaz *et al.*, 2010; Rao *et al.*, 2012). Furthermore, many oxides exhibit high magnetostriction coefficients ($CoFe_3O_4$, La(Sr)MnO_3) or high piezoelectric constants (PZT, PMN-PT, BTO) that makes them appealing for the design of various composite architectures where the magnetoelectric effects are mediated by strain. Strain coupling requires an optimum mechanical matching between the two constituent phases, which is sometimes very difficult to achieve in ceramics. For this reason, the effects are only observed in epitaxial composite films or patterned structures where the crystallographic orientation and interfacial roughness are accurately controlled. Nevertheless, even in epitaxially grown composite films, the changes in magnetization induced by voltage are typically rather low ($<5\%$), due to clamping effects with the substrate, which strongly limit the available strains.

Apart from the strain-mediated mechanism, an applied electric field can modulate the charge carrier density in oxide composite heterostructures, inducing noticeable changes in magnetization and coercivity. However, a direct demonstration of modulation of the magnetic properties in oxides heterostructures occurring through this mechanism remains relatively less explored (Schmitz-Antoniak *et al.*, 2013; Chu *et al.*, 2018). Furthermore, the presence of oxygen vacancies in the oxides has been shown to contribute to the magneto-ionic mechanism, where, as aforementioned, the voltage-driven oxygen ions migration can cause significant changes in coercivity, magnetization and magnetic anisotropy (Chien *et al.*, 2016). Various systems have been comprehensively analyzed and reviewed in recent articles (Song *et al.*, 2017; Chu *et al.*, 2018; Molinari *et al.*, 2019; Navarro-Senent *et al.*, 2019). In this section, we will focus specifically on the several oxide systems where the occurrence of nanoporosity has brought a significant contribution to the observed ME effects: Multiferroic $BiFeO_3$, solid state $CoFe_3O_4$/PZT, solid/liquid $CoFe_3O_4$/PC, and FeO_x/PC composites, and lithiated spinel ferrites.

The synthesis of the nanoporous oxides traditionally relies on the evaporation induced self-assembly (EISA) of the sol-gel type inorganic precursors and the amphiphilic diblock co-polymer templates, as depicted in **Fig. 4**. In aqueous or organic solvents, the precursors (e.g., metal chloride or nitrate) are hydrolysed and condensed to form inorganic polymers composed of M–O–M bonds (M is the metal). At the same time, the polymer forms micelles which attach to the metal ions (Step 1). During the dip-coating process, the polymer and sol-gel precursors are progressively concentrated by evaporation, leading to aggregation, gelation, and final drying to form a type of dry gel layer (Step 2). As a final step, the layers are heated in a controlled atmosphere in order to crystallize the oxide and burn out the polymer template which leaves behind the porous structure (Step 3). Remarkably, the nanoporous films can be also obtained directly by dip-coating, without the use of the polymer template (Robbennolt *et al.*, 2019b). In this case the degree of nanoporosity is governed by the solvent evaporation rate. A representative image of the FeO_x film produced by dip-coating in the absence of polymer template is also given in **Fig. 4**. This is a simple and relatively fast method to grow nanoporous oxide films with the controlled thickness, porosity and crystalline structure. More details on the methodology and the effect of the synthesis parameters can be found elsewhere (Schneller *et al.*, 2013; Zhang *et al.*, 2019; Galy *et al.*, 2020).

The mechanical flexibility brought by nanoporosity can provide a powerful tool to strain engineer nanostructured materials (Quickel *et al.*, 2010). The studies performed on internal multiferroic $BiFeO_3$ (Quickel *et al.*, 2015) revealed that the voltage-induced change in *d* spacing was 10 times greater than in the dense film of the same composition. However, it is not only the extent of the lattice strain that matters, but also the nature of strain. As the material is clamped to a rigid substrate, there is a gradient of strain (anisotropic strain) developed during the application of electric field. The strain symmetry lowering appears to be the key to the observed amplified voltage-induced magnetization of $BiFeO_3$, which exceeds the one of epitaxial $BiFeO_3$ systems. Indeed, the numerical results are impressive: upon electric field application the material shows a large change in saturation magnetization, from 0.04 to 0.84 μ_b per Fe, which is >20 times higher than in the dense sample.

This seminal work by Quickel *et al.*, paved a way towards the use of flexible nanoporous architectures for strain engineered ME composite materials. The later reports, where the pores are employed as a host to accommodate dielectric compounds, have proved the importance of nanoporosity for strain-engineered oxide systems. Nanoporous $CoFe_3O_4$ was produced using polymer templating of sol–gel derived thin films, followed by conformal filling the pores with a piezoelectric Pb(Zr,Ti)O_3 using atomic

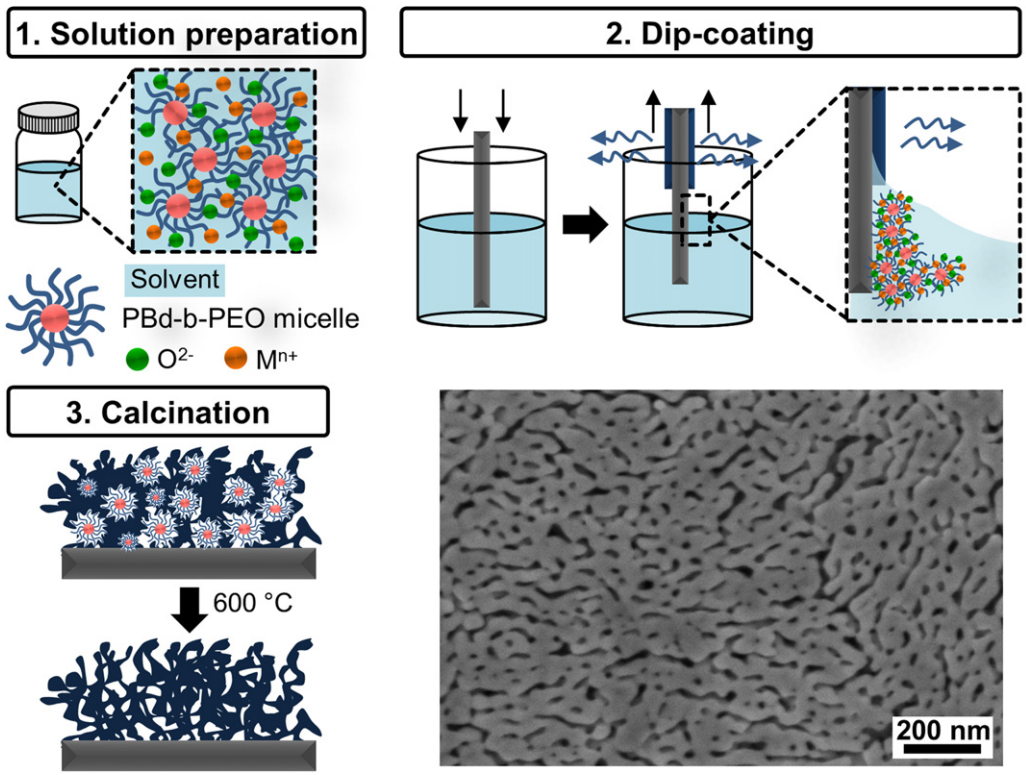

Fig. 4 Schematic pictures of the template-assisted sol–gel process used to induce nanoporosity in oxide films and a representative SEM image of nanoporous FeO_x layer obtained after calcination.

layer deposition, which resulted in a solid state composite ME material with a very high interfacial area (Chien *et al.*, 2016). Both materials are well documented in the literature and have generated significant interest due to their ferroic properties (Schmitz-Antoniak *et al.*, 2013; Rodzinski *et al.*, 2016; Paudel *et al.*, 2019). However, previous studies were focused on dense films where the magnetoelectric effects are significantly limited by substrate clamping and the effects of nanoporosity were mainly overlooked. In porous $CoFe_3O_4$ films grown on rigid substrates, the bottom of the layer remains clamped and therefore the in-plane strain is hindered. Nevertheless, the nanoporosity allows for out-of-plane flexing and thus, for more bond distortion in both $Pb(Zr,Ti)O_3$ and in the coupled $CoFe_3O_4$ as compared to dense films. Indeed, with the application of positive voltage, the most pronounced change in saturation magnetization was measured along the perpendicular-to-plane direction, that is, M_S increases by 15.4% (compared to 3.6% for in-plane measurements). Remarkably, the observed ME effects are reduced when the thickness of the $Pb(Zr,Ti)O_3$ increases. This again underscores the importance of the mechanical flexibility of the nanoporous frameworks, as thicker piezoelectric layer seals the pores, thus lowering the mechanical distortion and the strain transfer. However, the voltage-induced strain in $Pb(Zr,Ti)O_3$ is lost when the driving electric field is removed, that is, the observed effects are rather volatile.

Non-volatile, fully reversible electric-filed control of magnetism in nanoporous $CoFe_3O_4$ was achieved by magneto-ionic means, where a liquid electrolyte (propylene carbonate treated with metallic Na) was used to access the open porosity of the material (Robbennolt *et al.*, 2019a). Applying moderate negative voltage to the sample, between -10 and -50 V, causes a partial reduction of metal ions to zero valent state ($Co^{2+} \rightarrow Co^0$ and $Fe^{3+} \rightarrow Fe^{2+} \rightarrow Fe^0$) which is accompanied with the oxygen ions migration towards the surface or/and out of the sample. This leads to a maximum increase of M_S by 15% (see **Fig. 5**) and a decrease in H_C by 28% in the porous sample after applying -50 V. Analogous samples with lower porosity degree (synthesized by dip coating but without the diblock co-polymer) exhibit more modest magneto-ionic effects, that is, 2% increase in M_S and 4% decrease in H_C. This underscores the importance of nanoporosity in this system. The oxygen ion exchange between the sample and the liquid electrolyte occurs mainly at the solid/liquid interface, thus there are two main contributions from nanoporosity: (1) an enhanced overall interface area and (2) larger electric fields due to the reduced size of the ligaments (reduction of the effective thickness of the film since the electrolyte can penetrate towards the interior of the pores).

The way the oxygen ions are stored appears to be the key factor determining the reversibility of the magnetoelectric process. It has been demonstrated that the O^{2-} can be either dissolved in the electrolyte (Quintana *et al.*, 2018b; Robbennolt *et al.*, 2018) or aggregated at the grain boundaries forming oxides/hydroxides. In the case described above, that is, $CoFe_3O_4$/PC, the migratory oxygen was likely stored at the surface or at the grain boundaries which made it easier to reincorporate it back into the cobalt ferrite structure with the voltage of opposite polarity (Robbennolt *et al.*, 2019a). Indeed, a similar study performed on nanoporous FeO_x immersed in a liquid electrolyte demonstrated that the voltage-induced changes in M_S can be only partially reversed in the nanoporous sample when the oxygen ions are stored in the solution (Robbennolt *et al.*, 2019b). The O^{2-} ions can be stabilized by

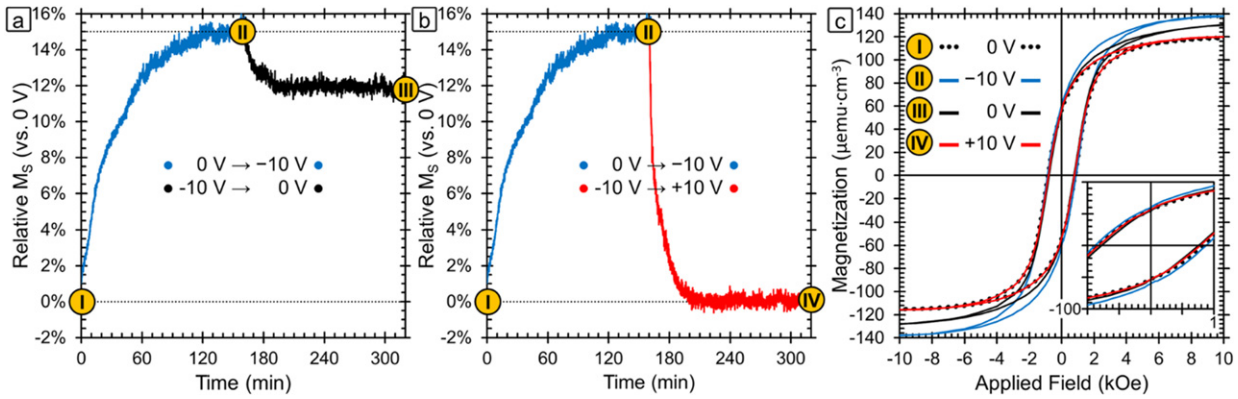

Fig. 5 (a) Relative change in saturation magnetization (M_S) vs. the initial sample magnetization as a function of time and applied voltage for nanoporous $CoFe_3O_4$ films. Point I is the initial sample as-synthesized. The blue line shows the evolution of the magnetization during the application of −10 V for 160 min and point II is the maximum magnetization reached. After the application of −10 V, the voltage was turned to 0 V (black line) in one case and +10 V (red line) in another, as it is shown in panel (b). Points III and IV are the sample state after the sample relaxed at 0 V and recovered under +10 V respectively. (c) Room-temperature magnetic hysteresis loops corresponding to points I–IV. The figure is reprinted from Robbennolt, S., Menéndez, E., Quintana, A., *et al.*, 2019a. Reversible, electric-field induced magneto-ionic control of magnetism in mesoporous cobalt ferrite thin films. Scientific Reports 9, 10804. doi:10.1038/s41598-019-46618-6.

polar solvent molecules and, depending on the voltage intensity, these ions remain in the electrolyte or become neutralized at the counter-electrode. In the latter case, the overall system loses part of the oxygen in form of bubbles which can make the magnetoelectric changes fully irreversible. In this case, the ability of the system to be re-oxidized will be dictated by the diffusion kinetics of the process.

Recently, magneto-ionic effects in spinel oxides have attracted the attention of scientists working on lithium ion batteries. Such materials ($LiFe_5O_8$, $CoFe_2O_4$, $NiFe_2O_4$, etc.) show ability to reversibly incorporate Li^+ ions from a liquid electrolyte and subsequently release these ions in a specific range of applied voltage (Reitz *et al.*, 2016; Dubraja *et al.*, 2018). Lithium intercalation causes a valence change and a partial redistribution of metal cations in the spinel structure, hence resulting in a large increase in magnetization at room temperature, that can be as high as 30% in some cases (Dasgupta *et al.*, 2014). Remarkably, magnetization reversal dictated by lithium intercalation mechanism is highly reversible (endurance of thousands of cycles), although only to a certain degree of lithiation, beyond which the original spinel structure cannot be fully recovered anymore. This is in line with the other works on oxides discussed previously in this article. Furthermore, the highly porous structure of these oxides allows for a reduced diffusion distance, while enhancing, to some extent, the mechanical resistivity of the material against failure due to volume changes (electrode breathing) during lithiation/de-lithiation.

Challenges and Perspectives

In recent years, exciting new results in the field of magnetoelectric actuation have been obtained in composites comprising metallic, semiconducting and dielectric nanoporous structures. The presence of nanoporosity allows for significant changes in the magnetic properties under application of moderate voltages. Furthermore, such systems are able to outperform at room temperature, compared to fully dense films with the same composition. This eventually leads to reduced energy cost and facile integration of these materials into devices. Indeed, there is a huge potential for these systems to be utilized in a myriad of energy-efficient applications: spintronic devices, energy harvesters, radio-frequency/microwave devices, non-invasive biomedical technologies, and neuromorphic computing platforms (Hu and Nan, 2019; Mishra *et al.*, 2019). Nevertheless, in most cases, the use of a liquid electrolyte is required to generate ultra-high electric fields (thanks to the formation of ultra-narrow electric double layers) and to access the large surface area of the complex 3D nanoporous networks (Navarro-Senent *et al.*, 2019). For further technological exploitation of these enhanced magnetoelectric effects it is important to fully adapt ME composites to operate in solid state. In fact, the pores can accommodate various host FE materials that can conformally coat the overall surface of highly porous FM phases, thus resulting in a new type of composite materials able to operate in all-solid state via magneto-ionic, strain-mediated or charge accumulation mechanisms, depending on the nature of the FM/FE materials. Particularly, there is large potential for nanoporous materials to be integrated in strain-mediated composites, for example, filling the pores with FE polymers to take advantage of the synergies between magnetostriction and piezoelectricity (e.g., PDVF (Martins *et al.*, 2015; Poddar *et al.*, 2018)), analogous to bioinspired three-dimensional magnetoactive scaffolds (Fernandes *et al.*, 2019). In addition, magneto-ionic control of magnetism can be achieved in nanoporous ME composites, where the guest material can be a solid electrolyte (ionic conductor) grown throughout the surface of the porous framework using, for example, ALD such as a high O^{2-} mobility thin film like Gd_2O_3

or HfO_2 (Detavernier *et al.*, 2011). In fact, it has been recently demonstrated that larger magneto-ionic effects can be obtained in nanoporous cobalt ferrite film conformally coated with HfO_2, as compared to a film having the same degree of porosity but simply immersed in an anhydrous electrolyte (Robbennolt *et al.*, 2020). Nevertheless, in this case, a liquid electrolyte was still employed during voltage application to avoid the problem of electrical pinholes in HfO_2. Furthermore, the magneto-ionic speed needs to be further increased, while keeping the reversibility and cyclability of the effects at room temperature. This challenge is being tackled by using hydrogen magneto-ionics instead of oxygen (Tan *et al.*, 2019), or optimizing the electric contacts and sample designs (de Rojas *et al.*, 2020). However, in spite of all these works, the mechanisms responsible for magnetoelectric actuation are, in general, still rather poorly understood.

Acknowledgments

Financial support by the European Research Council (SPIN-PORICS 2014-Consolidator Grant, Agreement No. 648454; MAGIC-SWITCH 2019-Proof of Concept Grant, Agreement No. 875018), the Spanish Government (MAT2017–86357-C3–1-R and associated FEDER) and the Generalitat de Catalunya (2017-SGR-292 and 2018-LLAV-00032) is acknowledged. Aliona Nicolenco is thankful to the European Commission for the financial support through the H2020-MSCA-IF-2019 project (Agreement No. 892661 – MAGNUS).

References

Ahmad, H., Atulasimha, J., Bandyopadhyay, S., 2015. Reversible strain-induced magnetization switching in FeGa nanomagnets: Pathway to a rewritable, non-volatile, non-toggle, extremely low energy straintronic memory. Scientific Reports 5. 18264. doi:10.1038/srep18264.

Bauer, U., Yao, L., Jun Tan, A., *et al.*, 2015. Magneto-ionic control of interfacial magnetism. Nature Materials 14 (2), 174–181. doi:10.1038/nmat4134.

Bibes, M., Villegas, J.E., Barthélèmy, A., 2011. Ultrathin oxide films and interfaces for electronics and spintronics. Advances in Physics 60 (1), 5–84. doi:10.1080/00018732.2010.534865.

Chen, X.Z., Hoop, M., Shamsudhin, N., *et al.*, 2017. Hybrid magnetoelectric nanowires for nanorobotic applications: Fabrication, magnetoelectric coupling, and magnetically assisted in vitro targeted drug delivery. Advanced Materials 29 (8), 1605458. doi:10.1002/adma.201605458.

Chiba, D., Yamanouchi, M., Matsukura, F., Ohno, H., 2003. Electrical manipulation of magnetization reversal in a ferromagnetic semiconductor. Science 301, 943–945. doi:10.1126/science.1086608.

Chien, D., Buditama, A., Schelhas, L., *et al.*, 2016. Tuning magnetoelectric coupling using porosity in multiferroic nanocomposites of ALD-grown $Pb(Zr,Ti)O_3$ and templated mesoporous $CoFe_2O_4$. Applied Physics Letters 109 (11), 112904. doi:10.1063/1.4962536.

Chu, Z., Pourhosseiniasl, M., Dong, S., 2018. Review of multi-layered magnetoelectric composite materials and devices applications. Journal of Physics D: Applied Physics 51 (24), 243001. doi:10.1088/1361-6463/aac29b.

Daalderop, G.H.O., Kelly, P.J., Schuurmans, M.F.H., 1991. Magnetocrystalline anisotropy and orbital moments in transition-metal compounds. Physical Review B 44 (21), 12054–12057. doi:10.1103/PhysRevB.44.12054.

Dasgupta, S., Das, B., Knapp, M., *et al.*, 2014. Intercalation-driven reversible control of magnetism in bulk ferromagnets. Advanced Materials 26 (27), 4639–4644. doi:10.1002/adma.201305932.

de Rojas, J., Quintana, A., Lopeandía, A., *et al.*, 2020. Boosting room temperature magneto-ionics in Co_3O_4. Science Advances. (Submitted).

Detavernier, C., Dendooven, J., Pulinthanathu Sree, S., Ludwigc, K., Martens, J., 2011. Tailoring nanoporous materials by atomic layer deposition. Chemical Society Reviews 40 (11), 5242–5253. doi:10.1039/c1cs15091j.

Dislaki, E., Robbennolt, S., Campoy-Quiles, M., *et al.*, 2018. Coercivity modulation in Fe–Cu pseudo-ordered porous thin films controlled by an applied voltage: A sustainable, energy-efficient approach to magnetoelectrically driven materials. Advanced Science 5 (8), 1800499. doi:10.1002/advs.201800499.

Drings, H., Viswanath, R., Kramer, D., *et al.*, 2006. Tuneable magnetic susceptibility of nanocrystalline palladium. Applied Physics Letters 88 (25), 253103. doi:10.1063/1.2216897.

Dubraja, L.A., Reitz, C., Velasco, L., *et al.*, 2018. Electrochemical tuning of magnetism in orderedmesoporous transition-metal ferrite films for micromagnetic actuation. ACS Applied Nano Materials 1 (1), 65–72. doi:10.1021/acsanm.7b00037.

Duschek, K., Pohl, D., Fähler, S., Nielsch, K., Leistner, K., 2016. Research update: Magnetoionic control of magnetization and anisotropy in layered oxide/metal heterostructures. APL Materials 4 (3), 032301. doi:10.1063/1.4942636.

Duschek, K., Petr, A., Zehner, J., Nielsch, K., Leistner, K., 2018. All-electrochemical voltage-control of magnetization in metal oxide/metal nanoislands. Journal of Materials Chemistry C 6 (31), 8411–8417. doi:10.1039/c8tc01994k.

Fernandes, M., Correia, D., Ribeiro, C., *et al.*, 2019. Bioinspired three-dimensional magneto-active scaffolds for bone tissue engineering. ACS Applied Materials & Interfaces 11, 45265–45275. doi:10.1021/acsami.9b14001.

Galy, T., Marszewski, M., King, S., *et al.*, 2020. Comparing methods for measuring thickness, refractive index, and porosity of mesoporous thin films. Microporous and Mesoporous Materials 29. 109677doi:10.1016/j.micromeso.2019.109677.

Ghosh, S., 2011. Charge-response of magnetization in nanoporous PdNi alloys. Journal of Magnetism and Magnetic Materials 323 (5), 552–556. doi:10.1016/j.jmmm.2010.10.008.

Ghosh, S., 2013. Switching magnetic order in nanoporous Pd–Ni by electrochemical charging. Journal of Materials Research 28 (21), 3010–3017. doi:10.1557/jmr.2013.291.

Ghosh, S., Lemier, C., Weissmüller, J., 2006. Charge-dependent magnetization in nanoporous Pd-Co alloys. IEEE Transactions on Magnetics 42 (10), 3617–3619. doi:10.1109/TMAG.2006.880922.

Gilbert, D.A., Olamit, J., Dumas, R., *et al.*, 2016. Controllable positive exchange bias via redox-driven oxygen migration. Nature Communications 7. 11050. doi:10.1038/ncomms11050.

Gößler, M., Albu, M., Klinser, G., *et al.*, 2019. Magneto-ionic switching of superparamagnetism. Small 15. 1904523. doi:10.1002/smll.201904523.

Heiligtag, F.J., Airaghi Leccardi, M., Erdem, D., Süess, M., Niederberger, M., 2014. Anisotropically structured magnetic aerogel monoliths. Nanoscale 6 (21), 13213–13221. doi:10.1039/c4nr04694c.

Hu, J.M., Nan, C.W., 2019. Opportunities and challenges for magnetoelectric devices. APL Materials 7 (8), 080905. doi:10.1063/1.5112089.

Ibrahim, F., Hallal, A., Dieny, B., Chshiev, M., 2018. Establishing characteristic behavior of voltage control of magnetic anisotropy by ionic migration. Physical Review B 98 (21), 214441. doi:10.1103/PhysRevB.98.214441.

Isarain-Chávez, E., Baro, M.D., Alcantara, C., *et al.*, 2018. Micelle-assisted electrodeposition of mesoporous Fe–Pt smooth thin films and their electrocatalytic activity towards the hydrogen evolution reaction. ChemSusChem 11 (2), 367–375. doi:10.1002/cssc.201701938.
Kharissova, O.V., Dias, H.V.R., Kharisov, B.I., 2015. Magnetic adsorbents based on micro- and nano-structured materials. RSC Advances 5 (9), 6695–6719. doi:10.1039/c4ra11423j.
Li, C., Iqbal, M., Lin, J., *et al.*, 2018. Electrochemical deposition: An advanced approach for templated synthesis of nanoporous metal architectures. Accounts of Chemical Research 51 (8), 1764–1773. doi:10.1021/acs.accounts.8b00119.
Liu, H., Yang, X., 2017. A brief review on perovskite multiferroics. Ferroelectrics 507 (1), 69–85. doi:10.1080/00150193.2017.1283171.
Martins, P., Gonçalves, R., Lopes, A.C., *et al.*, 2015. Novel hybrid multifunctional magnetoelectric porous composite films. Journal of Magnetism and Magnetic Materials 396, 237–241. doi:10.1016/j.jmmm.2015.08.041.
Mishra, A.K., Bansal, C., Ghafari, M., Kruk, R., Hahn, H., 2010. Tuning properties of nanoporous Au-Fe alloys by electrochemically induced surface charge variations. Physical Review B – Condensed Matter and Materials Physics 81 (15), 155452. doi:10.1103/PhysRevB.81.155452.
Mishra, R., Kumar, D., Yang, H., 2019. Oxygen-migration-based spintronic device emulating a biological synapse. Physical Review Applied 11 (5), 54065. doi:10.1103/PhysRevApplied.11.054065.
Molinari, A., Hahn, H., Kruk, R., 2018. Voltage-controlled on/off switching of ferromagnetism in manganite supercapacitors. Advanced Materials 30 (1), 1703908. doi:10.1002/adma.201703908.
Molinari, A., Hahn, H., Kruk, R., 2019. Voltage-control of magnetism in all-solid-state and solid/liquid magnetoelectric composites. Advanced Materials 31 (26), 1806662. doi:10.1002/adma.201806662.
Mushtaq, F., Chen, X., Torlakcik, H., *et al.*, 2019a. Magnetoelectrically driven catalytic degradation of organics. Advanced Materials 31. 1901378. doi:10.1002/adma.201901378.
Mushtaq, F., Torlakcik, H., Vallmajo-Martin, Q., *et al.*, 2019b. Magnetoelectric 3D scaffolds for enhanced bone cell proliferation. Applied Materials Today 16, 290–300. doi:10.1016/j.apmt.2019.06.004.
Navarro-Senent, C., Fornell, J., Isarain-Chávez, E., *et al.*, 2018. Large magnetoelectric effects in electrodeposited nanoporous microdisks driven by effective surface charging and magneto-ionics. ACS Applied Materials and Interfaces 10 (51), 44897–44905. doi:10.1021/acsami.8b17442.
Navarro-Senent, C., Quintana, A., Isarain-Chávez, E., *et al.*, 2020. Enhancing magneto-ionic effects in magnetic mesoporous films via conformal deposition of nanolayers with oxygen getter/donor capabilities. ACS Applied Materials and Interfaces 12 (12), 14484–14494. doi:10.1021/acsami.9b19363.
Navarro-Senent, C., Quintana, A., Menéndez, E., Pellicer, E., Sort, J., 2019. Electrolyte-gated magnetoelectric actuation: Phenomenology, materials, mechanisms, and prospective applications. APL Materials 7 (3), 030701. doi:10.1063/1.5080284.
Ohno, H., Chiba, D., Matsukura, F., *et al.*, 2000. Electric-field control of ferromagnetism. Nature 408 (6815), 944–946. doi:10.1038/35050040.
Paudel, B., Vasiliev, I., Hammouri, M., *et al.*, 2019. Strain vs. charge mediated magnetoelectric coupling across the magnetic oxide/ferroelectric interfaces. RSC Advances 9 (23), 13033–13041. doi:10.1039/c9ra01503e.
Peng, R.-C., Hu, J.M., Momeni, K., *et al.*, 2016. Fast 180° magnetization switching in a strain-mediated multiferroic heterostructure driven by a voltage. Scientific Reports 6, 27561. doi:10.1038/srep27561.
Poddar, S., de Sa, P., Cai, R., *et al.*, 2018. Room-temperature magnetic switching of the electric polarization in ferroelectric nanopillars. ACS Nano 12 (1), 576–584. doi:10.1021/acsnano.7b07389.
Quickel, T.E., Schelhas, L.T., Farrell, R.A., *et al.*, 2015. Mesoporous bismuth ferrite with amplified magnetoelectric coupling and electric field-induced ferrimagnetism. Nature Communications 6. 6562. doi:10.1038/ncomms7562.
Quickel, T.E., Le, V.H., Brezesinski, T., Tolbert, S.H., 2010. On the correlation between nanoscale structure and magnetic properties in ordered mesoporous cobalt ferrite ($CoFe_2O_4$) thin films. Nano Letters 10 (8), 2982–2988. doi:10.1021/nl1014266.
Quintana, A., Zhang, J., Isarain-Chávez, E., *et al.*, 2017. Voltage-induced coercivity reduction in nanoporous alloy films: A boost toward energy-efficient magnetic actuation. Advanced Functional Materials 27 (32), 1701904. doi:10.1002/adfm.201701904.
Quintana, A., Menéndez, E., Isarain-Chávez, E., *et al.*, 2018a. Tunable magnetism in nanoporous CuNi alloys by reversible voltage-driven element-selective redox processes. Small 14 (21), 1704396. doi:10.1002/smll.201704396.
Quintana, A., Menéndez, E., Liedke, M.O., *et al.*, 2018b. Voltage-controlled on-off ferromagnetism at room temperature in a single metal oxide film. ACS Nano 12, 10291–10300. doi:10.1021/acsnano.8b05407.
Rao, C.N.R., Sundaresan, A., Saha, R., 2012. Multiferroic and magnetoelectric oxides: The emerging scenario. Journal of Physical Chemistry Letters 3 (16), 2237–2246. doi:10.1021/jz300688b.
Reitz, C., Suchomski, C., Wang, D., Hahnad, H., Brezesinski, T., 2016. In situ tuning of magnetization via topotactic lithium insertion in ordered mesoporous lithium ferrite thin films. Journal of Materials Chemistry C 4 (38), 8889–8896. doi:10.1039/c6tc02731h.
Robbennolt, S., Menéndez, E., Quintana, A., *et al.*, 2019a. Reversible, electric-field induced magneto-ionic control of magnetism in mesoporous cobalt ferrite thin films. Scientific Reports 9. 10804. doi:10.1038/s41598-019-46618-6.
Robbennolt, S., Nicolenco, A., Mercier Fernandez, P., *et al.*, 2019b. Electric field control of magnetism in iron oxide nanoporous thin films. ACS Applied Materials and Interfaces 11, 37338–37346. doi:10.1021/acsami.9b13483.
Robbennolt, S., Yu, P., Nicolenco, A., *et al.*, 2020. Magneto-ionic control of magnetism in two-oxide nanocomposite thin films comprising mesoporous cobalt ferrite conformally nanocoated with HfO_2. Nanoscale 12, 5987–5994. doi:10.1039/c9nr10868h.
Robbennolt, S., Quintana, A., Pellicer, E., Sort, J., 2018. Large magnetoelectric effects mediated by electric-field-driven nanoscale phase transformations in sputtered (nanoparticulate) and electrochemically dealloyed (nanoporous) Fe-Cu films. Nanoscale 10 (30), 14570–14578. doi:10.1039/c8nr03924k.
Rodzinski, A., Guduru, R., Liang, P., *et al.*, 2016. Targeted and controlled anticancer drug delivery and release with magnetoelectric nanoparticles. Scientific Reports 6. 20867. doi:10.1038/srep20867
Schmitz-Antoniak, C., Schmitz, D., Borisov, P., *et al.*, 2013. Electric in-plane polarization in multiferroic $CoFe_2O_4/BaTiO_3$ nanocomposite tuned by magnetic fields. Nature Communications 4. 2051doi:10.1038/ncomms3051.
Schneller, T., Waser, R., Kosec, M., Payne, D. (Eds.), 2013. Chemical Solution Deposition of Functional Oxide Thin Films. Springer. pp. 1–796. doi:10.1007/978-3-211-99311-8.
Song, C., Cui, B., Li, F., Zhou, X., Pan, F., 2017. Recent progress in voltage control of magnetism: Materials, mechanisms, and performance. Progress in Materials Science 87, 33–82. doi:10.1016/j.pmatsci.2017.02.002.
Subkow, S., Fähnle, M., 2011. Potential explanation of charge response of magnetization in nanoporous systems. Physical Review B – Condensed Matter and Materials Physics 84 (22), 220409. doi:10.1103/PhysRevB.84.220409.
Sun, L., Chien, C.L., Searson, P.C., 2004. Fabrication of nanoporous nickel by electrochemical dealloying. Chemistry of Materials 16 (16), 3125–3129. doi:10.1021/cm0497881.
Tan, A.J., Huang, M., Avci, C.O., *et al.*, 2019. Magneto-ionic control of magnetism using a solid-state proton pump. Nature Materials 18 (1), 35–41. doi:10.1038/s41563-018-0211-5.
Topolovec, S., Jerabek, P., Vinga Szabó, D., Krenn, H., Würschum, R., 2013. SQUID magnetometry combined with in situ cyclic voltammetry: A case study of tunable magnetism of γ-Fe_2O_3 nanoparticles. Journal of Magnetism and Magnetic Materials 329, 43–48. doi:10.1016/j.jmmm.2012.09.071.
Torah, R.N., Beeby, S.P., White, N.M., 2004. Experimental investigation into the effect of substrate clamping on the piezoelectric behaviour of thick-film PZT elements. Journal of Physics D: Applied Physics 37 (7), 1074–1078. doi:10.1088/0022-3727/37/7/019.
Trewyn, B.G., Giri, S., Slowing, I.I., Lin, V.S.-Y., 2007. Mesoporous silica nanoparticle based controlled release, drug delivery, and biosensor systems. Chemical Communications. 3236–3245. doi:10.1039/b701744h.

Vaz, C.A.F., Hoffman, J., Ahn, C.H., Ramesh, R., 2010. Magnetoelectric coupling effects in multiferroic complex oxide composite structures. Advanced Materials 22 (26–27), 2900–2918. doi:10.1002/adma.200904326.

Wang, Y., Hu, J., Lin, Y., Nan, C.W., 2010. Multiferroic magnetoelectric composite nanostructures. NPG Asia Materials 2 (2), 61–68. doi:10.1038/asiamat.2010.32.

Weisheit, M., Fähler, S., Marty, A., *et al*., 2007. Electric field-induced modification of magnetism in thin-film ferromagnets. Science 315 (5810), 349–351. doi:10.1126/science.1136629.

Weissmüller, J., Viswanath, R.N., Kramer, D., *et al*., 2003. Charge-induced reversible strain in a metal. Science 300 (5617), 312–315. doi:10.1126/science.1081024.

Zhang, L., Jin, L., Liu, B., He, J., 2019. Templated growth of crystalline mesoporous materials: From soft/hard templates to colloidal templates. Frontiers in Chemistry 7, 22. doi:10.3389/fchem.2019.00022.

Zhang, Q., Lou, X., Wang, L., *et al*., 2016. Lithium-Ion battery cycling for magnetism control. Nano Letters 16 (1), 583–587. doi:10.1021/acs.nanolett.5b04276.

Zhou, X., Yan, Y., Jiang, M., *et al*., 2016. Role of oxygen ion migration in the electrical control of magnetism in Pt/Co/Ni/HfO_2 films. The Journal of Physical Chemistry C 120 (3), 1633–1639. doi:10.1021/acs.jpcc.5b10794.